ARTICLE

Substrate Independent Assembly of Optical Structures Guided by Biomolecular Interactions

Till Böcking,[†,‡,§] Kristopher A. Kilian,[‡] Peter J. Reece,[†] Katharina Gaus,[§] Michael Gal,[†] and J. Justin Gooding*[,‡]

School of Physics, School of Chemistry, and Centre for Vascular Research, University of New South Wales, Sydney, NSW 2052, Australia

ABSTRACT The chip-scale integration of optical components is crucial for technologies as diverse as optical communications, optoelectronics displays, and photovoltaics. However, the realization of integrated optical devices from discrete components is often hampered by the lack of a universal substrate for achieving monolithic integration and by incompatibilities between materials. Emergent technologies such as chip-scale biophotonics, organic optoelectronics, and optofluidics present a host of new challenges for optical device integration, which cannot be solved with existing bonding techniques. Here, we report a new method for substrate independent integration of dissimilar optical components by way of biological recognition-directed assembly. Bonding in this scheme is achieved by locally modifying the substrate with a protein receptor and the optical component with a biomolecular ligand or vice versa. The key features of this new technology include substrate independent assembly, cross-platform vertical scale integration, and selective registration of components based on complementary biomolecular interactions.

KEYWORDS: self-assembly • biomolecular interactions • porous silicon • photonic crystals • bonding • optical devices

One of the key elements of the success of the microelectronics industry over the past decades is the availability of a substrate that can provide full and scalable monolithic integration of electronic components. While the optoelectronics industry has made equally substantial progress over the same period at the component level, there is no clear convergence of competing platforms into one coherent technological framework. For example, silicon based photonics can be used to fabricate high quality optical circuits from passive elements such as photonic crystal waveguides, couplers, and resonators but lacks suitable active components such as light sources and modulators to create fully integrated systems. Technologies have been developed for integration of microcomponents via wafer-to-wafer transfer (1) or via fluidic self-assembly guided by complementary shape recognition, capillary forces, and hydrophobic interactions (2−6). These technologies, however, require time-consuming processing of the substrate: either precise etching of holes complementary to components (5) or photolithographic alignment and masking (7). Alternative methods require microfluidics to guide component assembly into microstructures, for example, by the use of railed microfluidic channels (8) or by controlling the flow inside a microfluidic chamber to direct components to target sites (9). Direct bonding attempts at vertical integration of different components are similarly labor intensive and fail to solve geometric compatibility issues (10−12). Moreover, the emergence of new technologies such as organic optoelectronics and nanocomposite semiconductor nanowires and quantum dots creates new integration issues, which are unlikely to be resolved using traditional microprocessing techniques and may well require new methods of fabricating devices.

Here, we report a technique for the integration of separate optical components together and onto various substrates, with minimal processing of that substrate, by way of biorecognition directed self-assembly. To demonstrate our biomolecular directed self-assembly method, free-standing silicon photonic crystal films are assembled at predetermined positions onto Si, GaAs, silica, and polycarbonate substrates. The bonding is achieved by locally modifying the substrate with a protein receptor and the optical component with a biomolecular ligand or vice versa. The high selectivity of the binding of conjugate molecular pairs ensures specific registration of components at the desired location. This advance provides a simple and flexible platform for vertical integration of separate optical materials and for the arraying of high quality optics based devices onto a wide range of substrates without compromising optical properties.

EXPERIMENTAL SECTION

Preparation of PSi and Lift-off. Si(100) wafer pieces (p++, B-doped, 0.005 ohm cm, single side polished) were cleaned by sonication in ethanol (2 × 10 min) and acetone (2 × 10 min) and blown dry under a stream of nitrogen. The cleaned wafer was etched in an electrochemical cell with a polished stainless steel electrode as back-contact and a Pt ring counter electrode using 25% ethanolic HF (mixture of 50% aqueous HF and

* Corresponding author. E-mail: Justin.Gooding@unsw.edu.au.
Received for review August 8, 2010 and accepted October 21, 2010
† School of Physics.
‡ School of Chemistry.
§ Centre for Vascular Research.
DOI: 10.1021/am1007084

Published on Web 11/05/2010

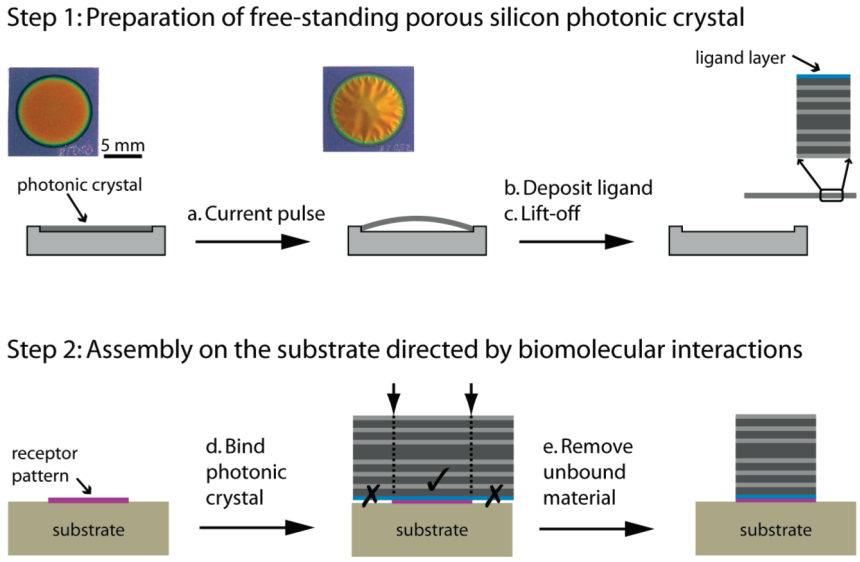

FIGURE 1. Schematic representation of the assembly of optical components by specific adhesion onto various substrates via biomolecular interactions. PSi optical resonant microcavities are prepared as free-standing films in the first step and then deposited via biorecognition-mediated self-assembly onto a substrate in the second step. The photographs show top views of an as prepared PSi photonic crystal (left) and a PSi photonic crystal after application of a current pulse (right). The resulting PSi film remains attached to the wafer around the edge, allowing modification with proteins on the top surface while the bottom surface remains unmodified. The modified PSi photonic crystal is then released and inverted onto a substrate of choice modified with a receptor pattern. Biorecognition between the ligand layer on the PSi film and the receptor pattern on the substrate results in strong bonding at the desired locations. The components are not drawn to scale; the thickness of the free-standing PSi photonic crystal is between 1.5 and 3 μm whereas the thickness of the combined ligand and receptor layer is in the order of 10 nm.

100% ethanol, 1:1, v/v) as electrolyte. The area of the silicon wafer in contact with the electrolyte solution (i.e., the etched area) was defined by an O-ring with an internal diameter of 1 cm. The power supply was controlled using a home-written software to modulate the current density and etching times during the etching process. Etch stops were incorporated into the etching program to allow recovery of the HF concentration at the etching front. The current densities and etch times required to obtain a PSi layer of desired porosity and thickness were calculated from calibration curves obtained for each batch of Si wafers and etching solutions. PSi films were lifted off the Si wafer using 15% ethanolic HF solution by application of a series of four to five short pulses of high current density (0.4 A cm^{-2}, 1 s pulses with 3 s break time between pulses). After lift-off, the sample was carefully rinsed with ethanol followed by pentane and dried under a very gentle stream of nitrogen with gentle heating (~40 °C).

Modification of PSi and Assembly Substrates with Protein. Proteins (avidin or biotinylated albumin) were deposited onto the hydrophobic surface of as-prepared PSi by physisorption from aqueous solution. The surface of as-prepared porous silicon is terminated in hydride species and, therefore, is hydrophobic. Aqueous solutions do not enter the hydrophobic pores of as-prepared PSi (Supplementary Figure S1, Supporting Information). The assembly substrates were spotted manually using a micropipettor with solutions of protein (1 mg mL^{-1}) to define the positions for adhesion, incubated for 10 min at room temperature in a humid chamber, and finally rinsed with water. Oxidation of the porous silicon was minimal during this short exposure to aqueous solutions. The resulting spots were typically 1 to 2 mm in diameter. Subsequently, poly(ethylene glycol) was physisorbed from aqueous solution elsewhere onto the substrate surface to diminish binding of the protein-modified lift-off sample to the bare substrate surface.

Assembly via Specific Biomolecular Interactions. The protein-modified lift-off sample (still attached at its edge to the underlying Si wafer) was removed from the Si wafer by scoring the edge of the PSi film with a sharp tip (scalpel) and floating the released PSi film off the Si wafer in a Petri dish filled with water. The free-standing photonic crystal was then picked up with a piece of filter paper, inverted onto the substrate, and allowed to interact with the protein spot. Finally, the film was vigorously rinsed with water and ethanol using a wash bottle to remove nonbound or weakly bound lift-off sample elsewhere on the substrate. Removal of avidin-modified float-off samples adhering nonspecifically to BSA-coated substrates required the use of detergent in the removal process.

Simulation of Reflectivity Spectra. The simulations are based on the effective medium formula by Looyenga (13), which has been validated for p++-type PSi (14). The starting parameters of the simulation (layer thickness and porosity) were taken from the etching program which calculates current density and etch times for a desired layer thickness and porosity from calibration curves. The values were then refined to achieve good agreement between the measured spectrum and the simulation. For a number of samples, the total thickness of the PSi sample was determined by profilometry to validate the layer thickness values used in the simulations.

RESULTS AND DISCUSSION

The strategy developed to self-assemble optical devices on a substrate of choice is shown in Figure 1. As proof of principle, we fabricate silicon based one-dimensional photonic band gap films (microcavities), delicate optical devices that can be easily tested and characterized, and attach them at predetermined positions on a number of different substrate materials. Porous silicon (PSi) photonic band gap films are suitable for the production of high quality optical (15−19) and biophotonics devices (20−22) that can be fabricated through a simple electrochemical etching process to define the refractive index profile of the film. The optical resonant microcavities prepared for this study consist of two distributed Bragg mirrors, each composed of alternating layers of low and high refractive index, separated by a low refractive index spacer layer. At the end of the electrochemical etching,

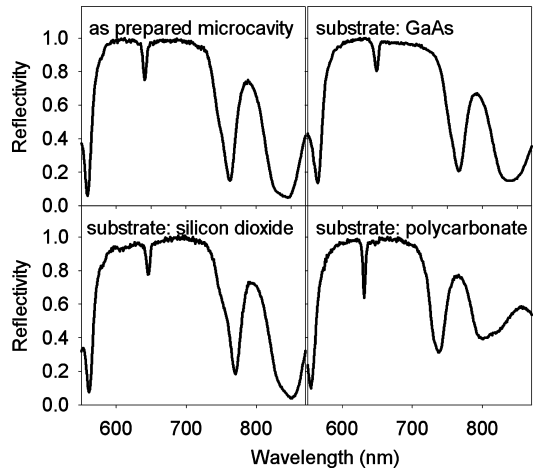

FIGURE 2. Measured reflectivity spectra of PSi microcavities before and after deposition onto GaAs, silicon dioxide, and polycarbonate.

we applied a high current pulse to "lift-off" the photonic film from the underlying Si wafer. As a result, the approximately 3 μm thick film becomes free-standing but remains attached to the Si wafer at the edges (see photographs of a PSi microcavity before and after application of the current pulse in Figure 1). The free-standing microcavity film can easily be modified by physisorption of a particular biorecognition element (e.g., a ligand) onto the exposed surface (Figure 1, Step b). The surface of freshly prepared PSi is terminated by hydride species and is hydrophobic, such that aqueous solutions do not enter the pores during the short exposure times (on the order of minutes; see Supplementary Figure S1, Supporting Information). Thus, the biorecognition element is selectively deposited onto the top surface whereas the bottom surface as well as the internal surfaces remain unaffected. Subsequently, the modified device is released from the Si wafer (Figure 1, Step c) and inverted onto the substrate of choice, which is premodified with a pattern of the complementary biomolecular species (e.g., a receptor) and passivated against nonspecific binding by treatment with poly(ethylene glycol) elsewhere on the surface. Portions of the freestanding PSi photonic crystal not bound to the substrate via the biorecognition pair can simply be washed away under a stream of water to leave microcavities only bound at positions determined by the receptor pattern on the substrate (Figure 1, Step e). The PSi structures deposited in this way retain their optical properties independent of the substrate. Figure 2 shows the characteristic optical reflectivity spectra of the same type of PSi microcavity assembled on GaAs, silicon dioxide, and polycarbonate, respectively, as directed by the interaction between the protein avidin on the device and spots of the complementary biotinylated bovine serum albumin (BSA) on the substrate. The reflection spectra of optical cavities are characterized by a sharp "dip" in the reflectivity at the resonant frequency in the Bragg plateau (the region of high reflectivity). The position and spectral width of the resonance is a sensitive measure of the structure and quality of the cavity. As can be seen, the cavity resonance is at approximately the same wavelength (within the variation of ~20 nm typically observed for the manufacturing process of our PSi crystals) (23) and has the same

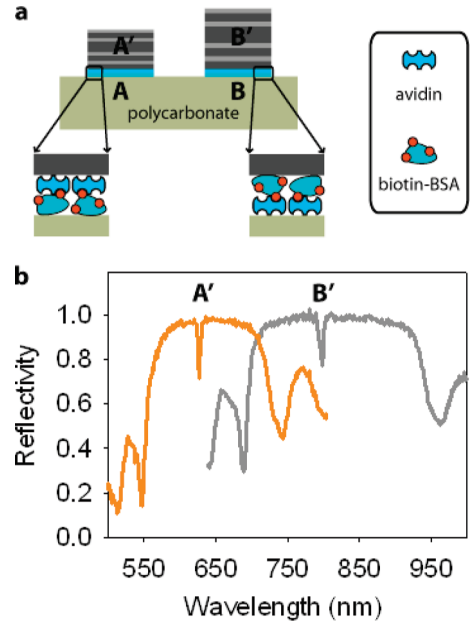

FIGURE 3. (a) Schematic illustration of the biomolecular scheme for depositing two different microcavities at defined positions on the substrate. (b) Measured reflectivity spectra of two different microcavities assembled on the same polycarbonate substrate as directed by biomolecular interactions.

width for all substrate types, thus showing that the cavity is largely impervious to the substrate. An advantage of this method is the possibility of depositing several components simultaneously without the need to individually align them at the desired locations on the substrate, as this task is performed by the biorecognition.

Another important benefit of the use of biorecognition is the possibility to self-assemble different types of optical components onto the same substrate using different biorecognition pairs. This concept is demonstrated in Figure 3 showing the attachment of two different microcavities with distinct resonant frequencies, onto different locations of the same substrate, which in this instance is a polycarbonate film. In this example, at location A the substrate is modified with avidin, while at location B the substrate is modified with biotinylated BSA. Two separate free-standing microcavities, A' and B', are modified with biotinylated BSA and avidin, respectively. Biorecognition, therefore, dictates that cavity A' assembles at position A, and similarly, the avidin modified cavity B' binds to the biotinylated substrate at location B. The deposition of the correct devices at their respective positions was verified by measuring their reflectivity spectra (Figure 3b). There were two important observations in performing this experiment. First, device B' did not assemble over spot A or vice versa (compare also Figure 7). Second, there is no need to align each optical device precisely with its respective receptor spot(s) on the substrate; unbound regions of the deposited free-standing structure simply break away during the washing step.

Biorecognition is also capable of self-assembling optical devices from separate components. To test this idea, PSi microcavities were assembled from two independent Bragg mirrors using biorecognition to create the desired resonant

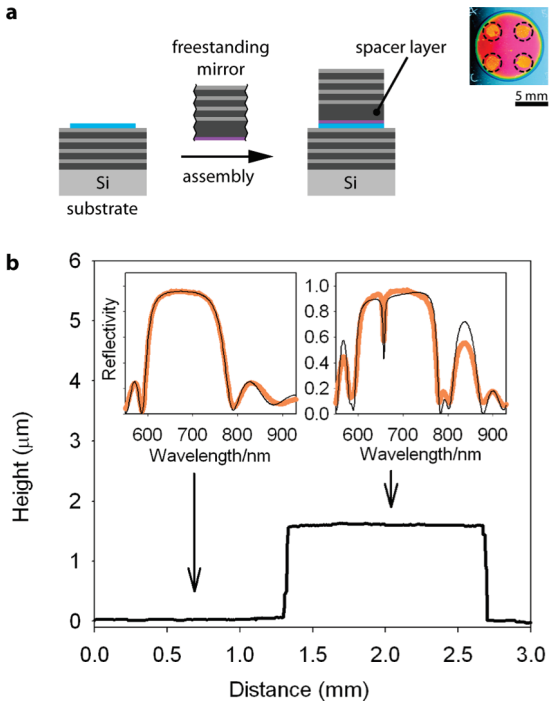

FIGURE 4. Assembly of microcavities from parts. (a) Schematic representation of the process: A free-standing Bragg mirror with spacer layer is bound to a substrate Bragg mirror via biomolecular interactions. The inset shows a photograph of a PSi substrate Bragg mirror with lift-off Bragg mirrors adhered at four locations (dotted circles) on the substrate. (b) Height profile of a bound sample. The insets show the measured reflectivity spectra (orange lines) of the underlying PSi Bragg mirror (left) and of the resonant microcavity (right) formed by the above-described method; the black lines represent simulations of the structures.

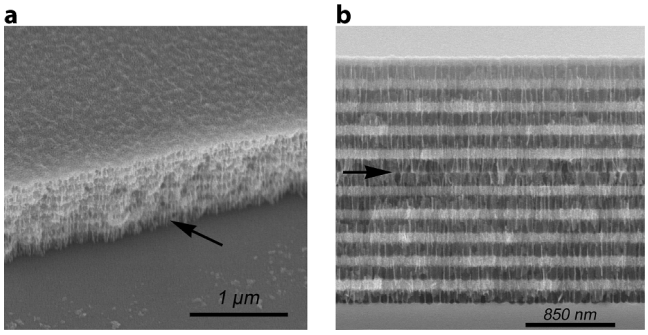

FIGURE 5. (a) SEM image showing the edge of a free-standing PSi Bragg mirror bound onto a substrate PSi Bragg mirror via biomolecular interactions. The deposited Bragg mirror consists of seven periods of alternating low and high porosity layers followed by a high porosity spacer layer (black arrow). (b) SEM image of a cross-section produced by cleaving a microcavity assembled via avidin–biotin interactions perpendicular to the surface. The arrow indicates the interface between the substrate Bragg mirror (bottom) and the deposited Bragg mirror (top).

cavities. The steps used are shown in Figure 4a: a free-standing PSi film consisting of a Bragg mirror and a spacer layer were placed onto a PSi Bragg mirror that was grown on the substrate. Biorecognition was used to mate the two parts to form the device. The scanning electron microscopy (SEM) image in Figure 5a shows the edge of a 1.5 μm thick PSi Bragg mirror film bound to a substrate mirror via biorecognition. The spacer layer of the microcavity (etched as an integral part of the free-standing mirror) is apparent

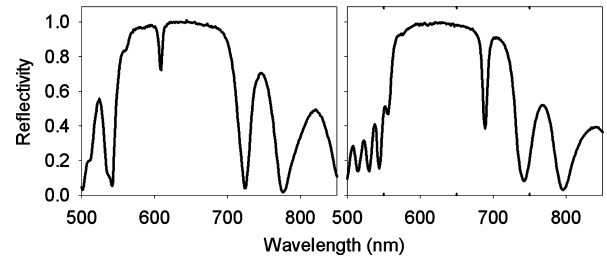

FIGURE 6. Measured reflectivity spectra of microcavities assembled with different optical thickness spacer layers (left: ~270 nm, right: ~400 nm) using the approach shown in Figure 4a.

as a distinct layer adjacent to the substrate (see arrow). The high and low porosity layers of such a structure and the uniform bonding between the substrate Bragg mirror and the deposited Bragg mirror are clearly visible in a cross-sectional SEM image of this type of structure (Figure 5b). The uniformity of the binding between the two components over a large length scale is also demonstrated in the profilometry trace (Figure 4b). The adhesion resulting from the multiple biomolecular interactions between the two optical components was sufficiently robust that the structures remained intact even after prolonged sonication in water or ethanol.

The assembly of microcavities was chosen to demonstrate the robustness and integrity of this biomolecular self-assembly approach as any nonuniformity in the produced spacer layer will result in poor optical characteristics. The successful assembly of the microcavity is confirmed by the appearance of a sharp cavity resonance at 660 nm in the reflectivity spectrum only at the location where the device was assembled (Figure 4b, inset). To further test this capability, we have fabricated cavities with spacer layers of different optical thickness (which can be achieved by varying either the thickness or the refractive index of the layer), and the cavity resonance was always in agreement with theoretical predictions. Figure 6 shows the reflectance spectra of microcavities fabricated on the same substrate with different thickness spacer layers giving rise to cavity resonances at 609 and 689 nm, respectively. Due to the high sensitivity of the optical properties of microcavities to relatively small changes in the spacer layer, the thickness of the bonding layer may have to be taken into account when designing and fabricating optical structures with this approach (see Supplementary Figure S2, Supporting Information).

Apart from being able to assemble or form high quality optical structures, the usefulness of the biomolecular self-assembly technique is determined by the success rate of forming the correct device in the correct location. Figure 7 provides details of the success rate of assembling the final microcavity. When the substrate reflector was modified with biotinylated BSA, 14 out of 15 avidin-modified lift-off reflectors correctly assembled into the specific microcavity. More importantly, when the substrate reflector was modified with a noncomplementary biomolecule, either with BSA alone (i.e., no conjugated biotin) or with avidin, then no microcavities were successfully assembled. Hence, the specific biological binding reaction is the necessary condition for device assembly.

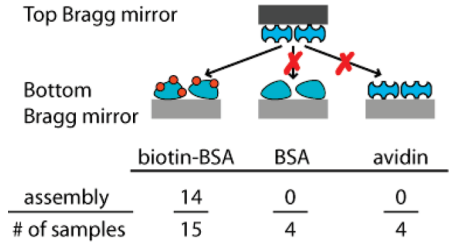

FIGURE 7. Assembly success rates showing the specificity of the assembly via biomolecular interactions.

We have shown that the affinity of biorecognition between biotin and avidin allows the alignment and assembly of high quality macroscale (>1 mm) photonic crystals. Biomolecules were deposited via manual spotting and adhered via simple physisorption without precise control over the density of the biomolecules on the surface. The structures assembled over these spots were dried out and remained bound in air at room temperature for several months. Future research into several key aspects is required to develop this proof-of-concept study toward mature technologies. First, the lateral resolution and connectivity of structures that can be achieved with this method needs to be determined. A second question concerns the long-term stability of the structures, especially when stored in air and at elevated temperatures, to assess whether the assembled device will need to be reinforced or encapsulated for long-term use. Surface chemistry approaches that tailor the reactivity and hydrophobicity of the substrate will aid the controlled immobilization of biomolecules and prevent nonspecific binding of components (24). Finally, the approach needs to be tested using other biorecognition reactions, including DNA duplex formation or antigen−antibody pairs, to guide different types of components to their specific locations on the substrate.

The high degree of strength and uniformity imparted with biorecognition and the prospect of shaping the assembled optical structure by removing unbound material should make the approach amenable to lithographic patterning. For instance, inkjet printing (25) or soft lithographic stamping (26) of proteins could define the circuit geography for the assembly of optical components. Patterning on flexible substrates and plastics could allow integration of optical components with advanced display (27, 28) and lab-on-a-chip (29) technologies. Furthermore, the approach could be expanded to other optical materials such that patterning different biomolecules for mixing different components could provide flexibility in design, especially when taking into account the wide range of surface functionality that can be introduced on semiconductors (e.g., via hydrosilylation chemistry for Si and PSi (30)), metals (31), and polymers (32). Individual optical devices can themselves be fabricated from different components and even different materials as demonstrated by incorporating separate spacer layers into microcavities. Thus, the composition (doping) of the spacer layer may be controlled entirely independently of that of the mirrors, which opens the door for new composite materials for diverse applications such as optical switches (33, 34) or biosensing at the cavity layer (20).

In summary, we have presented a novel method that utilizes biological recognition as a driving force for assembling optical components into more complex architectures on a range of substrates. With the continued need to develop robust and flexible strategies to incorporate photonic components into complex devices, this advance simplifies hybrid fabrication and expands current capabilities into composite materials such as sol−gel chemistry (35) and assembly of nanoparticles into photonic structures (36). In conjunction with the evolving landscape of lithographic techniques and nanofabrication, harnessing the power of nature's complexity with self-assembling systems will prove a powerful synergistic tool for technological advancement in the optoelectronics and photonics industries.

Acknowledgment. The authors thank Suhrawardi Ilyas for help with porous silicon fabrication. The research was supported under the Australian Research Council's Discovery Project's funding scheme (Project Number DO1094564).

Supporting Information Available: Reflectivity spectra of as-prepared PSi microcavities in air and immersed in water and ethanol; simulated reflectivity spectra showing the contribution of the biomolecular adhesion layer to the optical properties of the material. This material is available free of charge via the Internet at http://pubs.acs.org.

REFERENCES AND NOTES

(1) Schmidt, M. A. *Proc. IEEE* **1998**, *86* (8), 1575–1585.
(2) Srinivasan, U.; Liepmann, D.; Howe, R. T. *J. Microelectromech. Syst.* **2001**, *10* (1), 17–24.
(3) Jacobs, H. O.; Tao, A. R.; Schwartz, A.; Gracias, D. H.; Whitesides, G. M. *Science* **2002**, *296* (5566), 323–325.
(4) Clark, T. D.; Ferrigno, R.; Tien, J.; Paul, K. E.; Whitesides, G. M. *J. Am. Chem. Soc.* **2002**, *124* (19), 5419–5426.
(5) Stauth, S. A.; Parviz, B. A. *Proc. Natl. Acad. Sci. U.S.A.* **2006**, *103* (38), 13922–13927.
(6) Saeedi, E.; Kim, S.; Parviz, B. A. *J. Micromech. Microeng.* **2008**, *18* (7), 75019–75025.
(7) Judy, J. W. *Smart Mater. Struct.* **2001**, *10*, 1115–1134.
(8) Chung, S. E.; Park, W.; Shin, S.; Lee, S. A.; Kwon, S. *Nat. Mater.* **2008**, *7* (7), 581–587.
(9) Tolley, M. T.; Krishnan, M.; Erickson, D.; Lipson, H. *Appl. Phys. Lett.* **2008**, *93*, 254105.
(10) Mersali, B.; Ramdane, A.; Carenco, A. *IEEE J. Sel. Top. Quantum Electron.* **1997**, *3* (6), 1321–1331.
(11) Oktyabrsky, S.; Yakimov, M.; Tokranov, V.; van Eisden, J.; Katsnelson, A. *Proc. SPIE* **2005**, *5730*, 149–157.
(12) Roelkens, G.; Van Campenhout, J.; Brouckaert, J.; Van Thourhout, D.; Baets, R.; Romeo, P. R.; Regreny, P.; Kazmierczak, A.; Seassal, C.; Letartre, X.; Hollinger, G.; Fedeli, J. M.; Di Cioccio, L.; Lagahe-Blanchard, C. *Mater. Today* **2007**, *10* (7−8), 36–43.
(13) Looyenga, H. *Physica* **1965**, *31*, 401–406.
(14) Squire, E. K.; Snow, P. A.; Russell, P. S. J.; Canham, L. T.; Simons, A. J.; Reeves, C. L. *J. Lumin.* **1998**, *80* (1), 125–128.
(15) Chan, S.; Fauchet, P. M. *Appl. Phys. Lett.* **1999**, *75* (2), 274–276.
(16) Chan, S.; Fauchet, P. M. *Proc. SPIE* **1999**, *3630*, 144–154.
(17) Bruyant, A.; Lerondel, G.; Reece, P. J.; Gal, M. *Appl. Phys. Lett.* **2003**, *82* (19), 3227–3229.
(18) Ilyas, S.; Böcking, T.; Kilian, K.; Reece, P. J.; Gooding, J.; Gaus, K.; Gal, M. *Opt. Mater.* **2007**, *29* (6), 619–622.
(19) Reece, P. J.; Lerondel, G.; Zheng, W. H.; Gal, M. *Appl. Phys. Lett.* **2002**, *81* (26), 4895–4897.
(20) Ouyang, H.; DeLouise, L. A.; Miller, B. L.; Fauchet, P. M. *Anal. Chem.* **2007**, *79* (4), 1502–1506.
(21) Schwartz, M. P.; Derfus, A. M.; Alvarez, S. D.; Bhatia, S. N.; Sailor, M. J. *Langmuir* **2006**, *22* (16), 7084–7090.
(22) Kilian, K. A.; Böcking, T.; Gooding, J. J. *Chem. Commun.* **2009**, 630–640.

(23) Variations of the resonance peak position were observed across the surface of a PSi photonic crystal as well as between different samples. These variations presumably result from inhomogeneities and fluctuations in the current density and electrolyte composition.
(24) Böcking, T.; Kilian, K. A.; Gaus, K.; Gooding, J. J. *Langmuir* **2006**, *22* (8), 3494–3496.
(25) Barbulovic-Nad, I.; Lucente, M.; Sun, Y.; Zhang, M.; Wheeler, A. R.; Bussmann, M. *Crit. Rev. Biotechnol.* **2006**, *26* (4), 237–259.
(26) Wolfe, D. B.; Whitesides, G. M. In *Nanolithography and Patterning Techniques in Microelectronics*; Bucknall, D., Ed.; Woodhead Publishing: Cambridge, 2005; pp 76—119.
(27) Chen, Y.; Au, J.; Kazlas, P.; Ritenour, A.; Gates, H.; McCreary, M. *Nature* **2003**, *423* (6936), 136.
(28) Arsenault, A. C.; Puzzo, D. P.; Manners, I.; Ozin, G. A. *Nat. Photonics* **2007**, *1*, 468–472.
(29) Bartos, H.; Goetz, F.; Peters, R.-P. *Nanobiotechnology* **2004**, 13–30.
(30) Buriak, J. M. *Chem. Rev.* **2002**, *102* (5), 1271–1308.
(31) Witt, D.; Klajn, R.; Barski, P.; Grzybowski, B. A. *Curr. Org. Chem.* **2004**, *8* (18), 1763–1797.
(32) Ruckenstein, E.; Li, Z. F. *Adv. Colloid Interface Sci.* **2005**, *113* (1), 43–63.
(33) Moritsugu, M.; Kim, S. N.; Ogata, T.; Nonaka, T.; Kurihara, S.; Kubo, S.; Segawa, H.; Sato, O. *Appl. Phys. Lett.* **2006**, *89* (15), 153131/1–153131/3.
(34) Cross, G. *Laser Focus World* **2003**, *39* (5), 150–152.
(35) Jasieniak, J.; Sada, C.; Chiasera, A.; Ferrari, M.; Martucci, A.; Mulvaney, P. *Adv. Funct. Mater.* **2008**, *18* (23), 3772–3779.
(36) Puzzo, D. P.; Bonifacio, L. D.; Oreopoulos, J.; Yip, C. M.; Manners, I.; Ozin, G. A. *J. Mater. Chem.* **2009**, *19* (21), 3500–3506.

AM1007084